Polyhedron 135 (2017) 79–85

Contents lists available at ScienceDirect

Polyhedron

journal homepage: www.elsevier.com/locate/poly

Modulation of the absorption properties of a novel iron trisbipyridyl complex by introducing peripheral ruthenium ammines

Juan H. Mecchia Ortiz, Néstor E. Katz *

INQUINOA-UNT-CONICET, Instituto de Química Física, Facultad de Bioquímica, Química y Farmacia, Universidad Nacional de Tucumán, Ayacucho 471, T4000INI San Miguel de Tucumán, Argentina

ARTICLE INFO

Article history:
Received 3 April 2017
Accepted 30 June 2017
Available online 8 July 2017

Keywords:
Mixed-Valence
Iron bipyridyls
Ruthenium ammines
Intervalence charge transfer
NIR absorption

ABSTRACT

The novel trisbipyridyl iron complex of formula $[Fe(Mebpy\text{-}CN)_3](PF_6)_2$ (**1**) (with Mebpy-CN = 4-methyl-2,2′-bipyridine-4′-carbonitrile) and three novel heteropolynuclear complexes of formulae: $[(Mebpy\text{-}CN)_2Fe(Mebpy\text{-}CN)Ru(NH_3)_5](PF_6)_4$ (**2**), $[(Mebpy\text{-}CN)Fe\{(Mebpy\text{-}CN)Ru(NH_3)_5\}_2](PF_6)_6$ (**3**) and $[Fe\{(Mebpy\text{-}CN)Ru(NH_3)_5\}_3](PF_6)_8$ (**4**), were synthesized and characterized by spectroscopic and electrochemical techniques. When introducing peripheral ruthenium ammines to complex (**1**) using Mebpy-CN as a bridging ligand in complexes (**2**) to (**4**), the molar absorptivities increase in the visible region with increasing nuclearity of the complex. When oxidizing the Ru centers in the heteropolynuclear species, the corresponding three mixed-valent species are obtained, displaying IVCT (intervalence charge transfer) bands at λ_{max} = 850 nm, with molar absorptivities that are also enhanced by increasing the number of pentaammineruthenium moieties. The modulation of the absorption properties of transition metal complexes in the visible and NIR regions is a relevant issue for improving the performance of Dye-Sensitized Solar Cells, since their efficiency can be enlarged with increasing absorption in these regions.

1. Introduction

Since the discovery of the Creutz-Taube ion [1], mixed-valent complexes have been extensively studied for testing intramolecular electron transfer theories, an area which has considerably expanded since the pioneering studies on electron transfer by Marcus [2] and Hush [3]. Besides, multinuclear species have attracted interest in the area of artificial photosynthesis [4].

In a previous work [5], we have described the preparation and characterization of novel mixed-valent complexes containing ruthenium bipyridyls and ruthenium ammines bridged by Mebpy-CN (=4-methyl-2,2′-bipyridine-4′-carbonitrile); a considerable interaction was disclosed between both metallic centers.

In this work, we report the synthesis and physicochemical properties of a novel trisbipyridyl iron complex of formula $[Fe(Mebpy\text{-}CN)_3](PF_6)_2$ (**1**) and three heteropolynuclear complexes of formulae: $[(Mebpy\text{-}CN)_2Fe(Mebpy\text{-}CN)Ru(NH_3)_5](PF_6)_4$ (**2**), $[(Mebpy\text{-}CN)Fe\{(Mebpy\text{-}CN)Ru(NH_3)_5\}_2](PF_6)_6$ (**3**) and $[Fe\{(Mebpy\text{-}CN)Ru(NH_3)_5\}_3](PF_6)_8$ (**4**), which were obtained by introducing peripheral ruthenium ammines to complex (**1**) and using Mebpy-CN as a bridging ligand. The proposed structures of the cations of these complexes are shown in Scheme 1. Oxidation of the ruthenium(II) centers in complexes (**2**)–(**4**) leads to the corresponding mixed-valent species, that can be used as models for studying intramolecular electron transfer processes in multinuclear complexes.

2. Experimental

2.1. Materials and methods

All chemicals used in this work were analytical-reagent grade. CH_3CN was freshly distilled over P_4O_{10} for electrochemical measurements. Infrared spectra were measured as KBr pellets in the 4000–400 cm^{-1} range, with a Perkin-Elmer FTIR RX-I spectrophotometer. Raman spectra were recorded in the range 3500–60 cm^{-1} with a Raman DXR spectrometer from Thermo Scientific, equipped with a trinocular Olympus Microscope, sited at the LERA's facilities (CONICET-UNT). This equipment has available lasers at 780 and 532 nm. Electrochemical measurements were carried out using a BAS Epsilon EC potentiostat/galvanostat. A standard three-electrode arrangement was used, with vitreous carbon as working electrode, Pt wire as auxiliary electrode, and Ag/AgCl (3 M KCl) as reference electrode. All solutions were prepared in freshly distilled CH_3CN, with tetra-*n*-butylammonium hexafluorophosphate (TBAH) as the supporting electrolyte, and thoroughly

* Corresponding author.
E-mail address: nkatz@fbqf.unt.edu.ar (N.E. Katz).

http://dx.doi.org/10.1016/j.poly.2017.06.051
0277-5387/

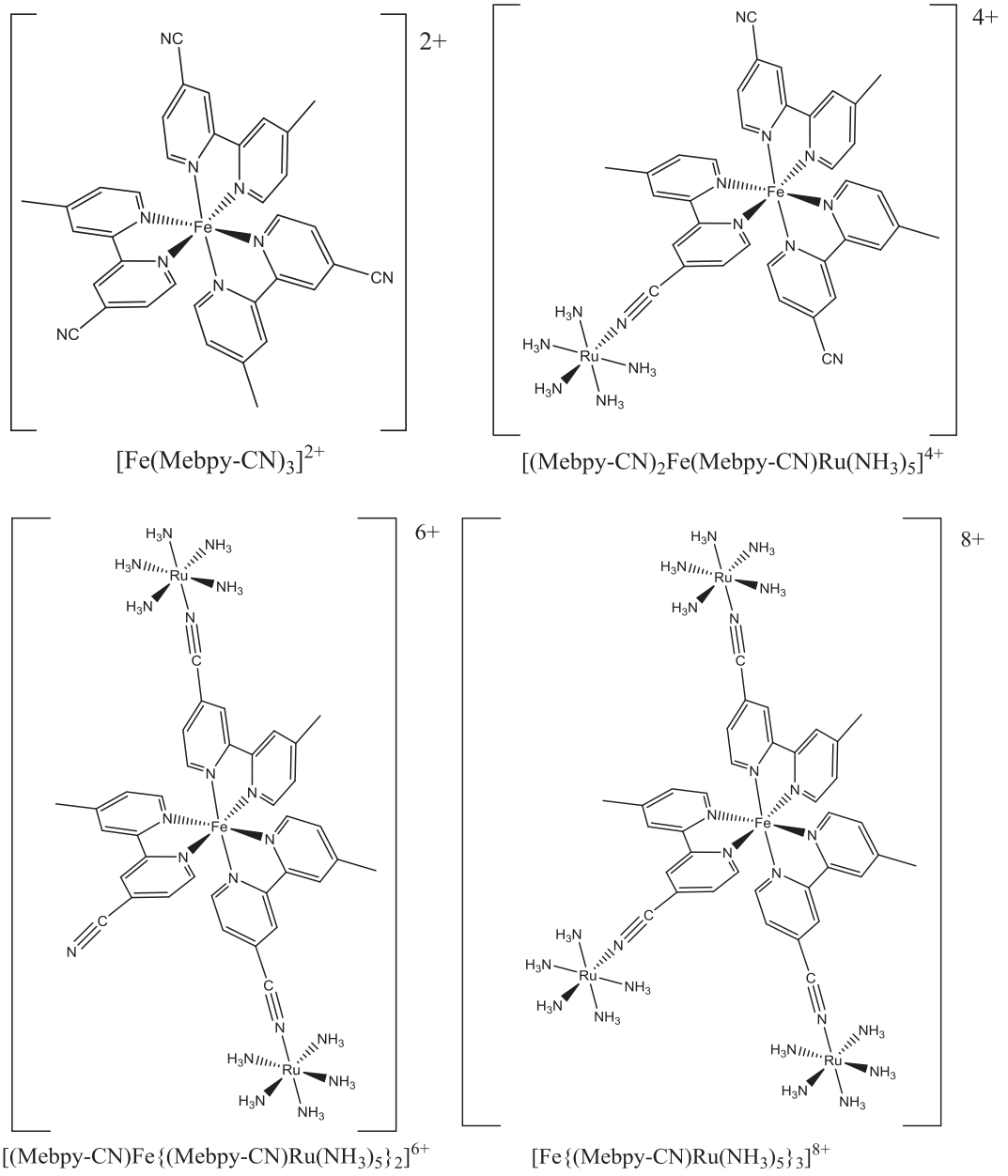

Scheme 1. Structure of the cations of complexes (**1**)–(**4**).

degassed with Ar prior to each measurement. Reported $E_{½}$ values were calculated as the averages between the peak values corresponding to the cathodic (E_c) and anodic (E_a) waves: $E_{½} = (E_c + E_a)/2$. Data obtained by cyclic voltammetry (CV) were almost equal to those obtained by differential pulse voltammetry (DPV). UV–Vis absorption spectra were recorded on a Varian Cary 50 spectrophotometer using 1-cm quartz cells. UV–Vis spectroelectrochemical experiments were performed in CH_3CN (0.1 M TBAH) using a 1-mm path length spectroelectrochemical cell (CH Instruments) with Pt grid as working electrode, Pt wire as counter electrode, and Ag/AgCl (3 M KCl) as reference electrode. Bromine solutions in CH_3CN were standardized by using $\varepsilon = 183\ M^{-1}\ cm^{-1}$ at $\lambda = 392$ nm [6]. Dinuclear complex (**2**) was prepared in acetone, using solid PF_6^- salts as precursors, while complexes (**3**) and (**4**) were obtained in water, using aqueous soluble precursors, considering that the higher dielectric constant of water – as compared to acetone – improves the synthesis of highly charged species.

2.2. Synthesis of $[Fe(Mebpy\text{-}CN)_3](PF_6)_2{\cdot}2.5H_2O$ (**1**)

100 mg (0.504 mmol) of Mebpy-CN – prepared as in our previous work [5] – dissolved in 3 mL of warm methanol were added to 10 mL of an aqueous solution of 43 mg (0.154 mmol) of $FeSO_4{\cdot}7H_2O$ and a spatula tip of ascorbic acid. After 30 min of stirring at room temperature, the solution turned from a light green to a dark purple color. It was then filtered to remove a small quantity of unreacted ligand. To the filtrate, 500 mg of NH_4PF_6 dissolved in 2 mL of water were added and the mixture was stored in the refrigerator during 4 h. The obtained purple solid was filtered, washed with cold water (3 × 5 mL) and ether (3 × 5 mL), and stored under vacuum over P_4O_{10} for 1 day. Yield: 66 mg (46%). Chemical analyses were coherent with the formula $[Fe(Mebpy\text{-}CN)_3](PF_6)_2{\cdot}2.5H_2O$. *Anal.* Calc. for $C_{36}H_{32}F_{12}N_9O_{2.5}P_2Fe$: C, 44.3; H, 3.3; N, 12.9. Found: C, 44.6; H, 3.1; N, 12.5. UV–Vis (CH_3CN) λ/nm ($\varepsilon \times 10^{-4}/M^{-1}\ cm^{-1}$): 254 (2.20), 307 (3.54), 353 (0.38), 546 (0.90).

2.3. Synthesis of [(Mebpy-CN)$_2$Fe(Mebpy-CN)Ru(NH$_3$)$_5$](PF$_6$)$_4$·8H$_2$O (**2**)

A solution of 109 mg (0.112 mmol) of (**1**) in acetone (20 mL) was purged with Ar for 30 min. Then, 67 mg (0.136 mmol) of [Ru(NH$_3$)$_5$(H$_2$O)](PF$_6$)$_2$ (prepared according to a reported method [7]) was added, and the resulting mixture was stirred under Ar for 4 h. The solution was concentrated to *ca.* 5 mL, and 50 mL of ether was added to precipitate a dark-purple solid, which was stored overnight. The solid was filtered, rinsed with ether, and purified by chromatography in Sephadex LH-20 (dichloromethane:acetone:methanol, 4:3:1). The unreacted ruthenium mononuclear precursor eluted first, while the new dinuclear complex was collected afterwards, rotoevaporated to dryness, recrystallized in acetone:dichloromethane and stored in the refrigerator overnight. No evidence of the formation of compounds of higher nuclearity as by-products was obtained. The obtained dark-purple solid was filtered and dried under vacuum over P$_4$O$_{10}$. Yield: 115 mg (66%). Chemical analyses were coherent with the formula [(Mebpy-CN)$_2$Fe(Mebpy-CN)Ru(NH$_3$)$_5$](PF$_6$)$_4$·8H$_2$O. *Anal.* Calc. for C$_{36}$H$_{58}$F$_{24}$FeN$_{14}$O$_8$P$_4$Ru: C, 27.8; H, 3.7; N, 12.7. Found: C, 27.3; H, 3.1; N, 13.2. IR (KBr, cm^{-1}): 3437(m), 3367 (m), 2929(vw), 2241(vw), 2178(s), 1623 (m), 1608(m), 1414(w), 1288 (w), 833(vs), 559(s). UV–Vis (CH$_3$CN) λ/nm (ε × 10^{-4}/M^{-1} cm^{-1}): 255 (2.97), 308 (3.97), 353 (0.46), 477 (1.07), 573 (1.85).

2.4. Synthesis of [(Mebpy-CN)Fe{(Mebpy-CN)Ru(NH$_3$)$_5$}$_2$](PF$_6$)$_6$·3CH$_3$CN·3CH$_3$OH (**3**)

5 mL of an aqueous solution of [Fe(Mebpy-CN)$_3$](SO$_4$), prepared by mixing 50 mg (0.252 mmol) of Mebpy-CN and 22 mg (0.079 mmol) of FeSO$_4$·7H$_2$O and a spatula tip of ascorbic acid, was purged with Ar during 30 min. Then, 5 mL of an aqueous solution of [Ru(NH$_3$)$_5$(H$_2$O)]Cl$_2$, prepared by reducing 50 mg (0.171 mmol) of [Ru(NH$_3$)$_5$Cl]Cl$_2$ by Zn amalgam, was added with an oxygen-free syringe. The solution was stirred under Ar for 6 h, and then 2 mL of a concentrated aqueous solution of NH$_4$PF$_6$ was added. The solid was filtered, washed with cold water (3 × 5 mL) and ether (3 × 10 mL) and dried under vacuum over P$_4$O$_{10}$. The obtained solid was purified by chromatography in Sephadex LH-20 (acetonitrile:methanol, 5:1); the collected fraction was rotoevaporated to 5 mL, precipitated with ether and stored in the refrigerator overnight. The solid was filtered, washed with ether and dried under vacuum over P$_4$O$_{10}$. Yield: 100 mg (60%). Chemical analyses were coherent with the formula [Mebpy-CN)Fe{(Mebpy-CN)Ru(NH$_3$)$_5$}$_2$](PF$_6$)$_6$·3CH$_3$CN·3CH$_3$COH. *Anal.* Calc. for C$_{45}$H$_{78}$F$_{36}$N$_{22}$O$_3$P$_6$FeRu$_2$: C, 14.6; H, 3.7; N, 14.6. Found: C, 14.1; H, 3.6; N, 14.1. IR (KBr, cm^{-1}): 3430(m), 3367 (m), 2929(vw), 2240(vw), 2181(s), 1624 (w), 1608(m), 1414(vw), 1290(w), 835 (vs), 559(m). UV–Vis (CH$_3$CN) λ/nm (ε × 10^{-4}/M^{-1} cm^{-1}): 254 (4.35), 307 (4.38), 360 (0.70), 490 (1.86), 574 (2.81).

2.5. Synthesis of [Fe{(Mebpy-CN)Ru(NH$_3$)$_5$}$_3$](PF$_6$)$_8$·2H$_2$O (**4**)

5 mL of an aqueous solution of [Fe(Mebpy-CN)$_3$](SO$_4$), prepared by mixing 60 mg (0.307 mmol) of Mebpy-CN and 26 mg (0.093 mmol) of FeSO$_4$·7H$_2$O and a spatula tip of ascorbic acid, was purged with Ar during 30 min. Then, 10 mL of an aqueous solution of [Ru(NH$_3$)$_5$(H$_2$O)]Cl$_2$, prepared by reducing 95 mg (0.325 mmol) of [Ru(NH$_3$)$_5$Cl]Cl$_2$ with Zn amalgam, was added with an oxygen- free syringe. The solution was stirred under Ar for 8 h. The solution was rotoevaporated to a minimum volume and stored in the refrigerator. The mixture was purified by chromatography in Sephadex G-25, and the collected fraction was rotoevaporated to *ca.* 10 mL and precipitated by adding 2 mL of a concentrated aqueous solution of NH$_4$PF$_6$. The solid was filtered, washed with cold water (3 × 5 mL) and ether (3 × 10 mL) and dried under vacuum over P$_4$O$_{10}$. Yield: 120 mg (54%). Chemical analyses were coherent with the formula [Fe{(Mebpy-CN)Ru(NH$_3$)$_5$}$_3$](PF$_6$)$_8$·2H$_2$O. *Anal.* Calc. for C$_{36}$H$_{76}$F$_{48}$N$_{24}$O$_2$P$_8$FeRu$_3$: C, 18.1; H, 3.2; N, 14.1. Found: C, 18.5; H, 3.2; N, 13.5. IR (KBr, cm^{-1}): 3433(m), 3367 (m), 2930(vw), 2181(s), 1623 (w), 1608 (w), 1414(vw), 1290(w), 837(vs), 559(m). UV–Vis (CH$_3$CN) λ/nm (ε × 10^{-4}/M^{-1} cm^{-1}): 254 (5.73), 307 (5.49), 363 (0.94), 495 (2.58), 581 (3.80).

3. Results and discussion

Stereochemistry in octahedral metal complexes with bidentate ligands has already been analyzed in detail by Keene [8]. It is well known that overcrowding pyridyl rings lead to steric hindrance; therefore, it is expected that *trans*-isomers of the multinuclear species will be less sterically demanding than the *cis*-isomers, so that the structures shown in Scheme 1 are probably the most stable ones. The possible existence of geometric isomers has also been described in similar complexes, although no evidence of differences in their physicochemical properties have been assessed; it is therefore assumed that the reported spectroscopic and electrochemical data represent an average of the various possible isomers for all the complexes.

3.1. IR spectra

The IR spectra of complexes (**1**)–(**4**) exhibit the typical vibrational modes of the polypyridyl ligands between 1650 and 1400 cm^{-1} and the characteristic band corresponding to the C≡N stretching mode of Mebpy-CN, ν(C≡N) [5]. As shown in Fig. 1, above, the IR spectrum of (**1**) has a low-intensity band at ν(C≡N) = 2242 cm^{-1}, which is displaced 8 cm^{-1} to higher wavenumbers with respect to that of the free ligand. The corresponding value observed in the related complex [Ru(Mebpy-CN)$_3$](PF$_6$)$_2$·0.5H$_2$O [5], is also displaced to higher frequencies when compared to the free ligand value ($\Delta\nu$ = 6 cm^{-1}). These small shifts can be attributed to metal coordination to the pyridinic nitrogens of Mebpy-CN. In contrast, complexes (**2**) to (**4**) display very intense nitrile stretching bands at an average value of ν(C≡N) = 2180 cm^{-1}, as shown in Fig. 1, below, which is considerably shifted to a lower value respect to that of the free ligand ($\Delta\nu$ = −54 cm^{-1}) as a consequence of the strong π- backbonding effect from d_π orbitals of ammine Ru to π* orbitals of the nitrile moiety of Mebpy-CN. The same phenomenon is observed in related dinuclear complexes that include Mebpy-CN as a bridging ligand between Ru or Re moieties and pentaammineruthenium(II) groups ($\Delta\nu$ = −58 cm^{-1} and $\Delta\nu$ = −55 cm^{-1} respectively [5,9]). Complexes (**2**) to (**4**) also display the characteristic ammonia symmetric deformation mode at an average value: δ_{sym}(NH$_3$) = 1289 cm^{-1}, a clear indication of oxidation state (II) for ruthenium [10].

3.2. Raman spectra

As described below in the UV–Vis section, the intense band at λ_{max} = 546 nm observed for complex (**1**) is assigned to a MLCT (metal-to-ligand charge transfer) d_π (Fe) → π* (Mebpy-CN). In Fig. 2, the IR spectrum of (**1**) is compared to its Resonance Raman (RR) spectrum (recorded by using a 532 nm laser) and to its Raman spectrum (obtained by using a 780 nm laser). In the RR spectrum, the intensities of the bands at 2239, 1611, 1482, 1275 and 1019 cm^{-1} are considerably enhanced. These modes are related to the symmetric C=N and C=C stretching vibrations from the pyridine rings, as supported by comparison to related bands of the parent complex [Fe(bpy)$_3$]$^{2+}$ [11]. In the RR spectrum, there is a remarkable increment of the intensity of the band at 2239 cm^{-1},

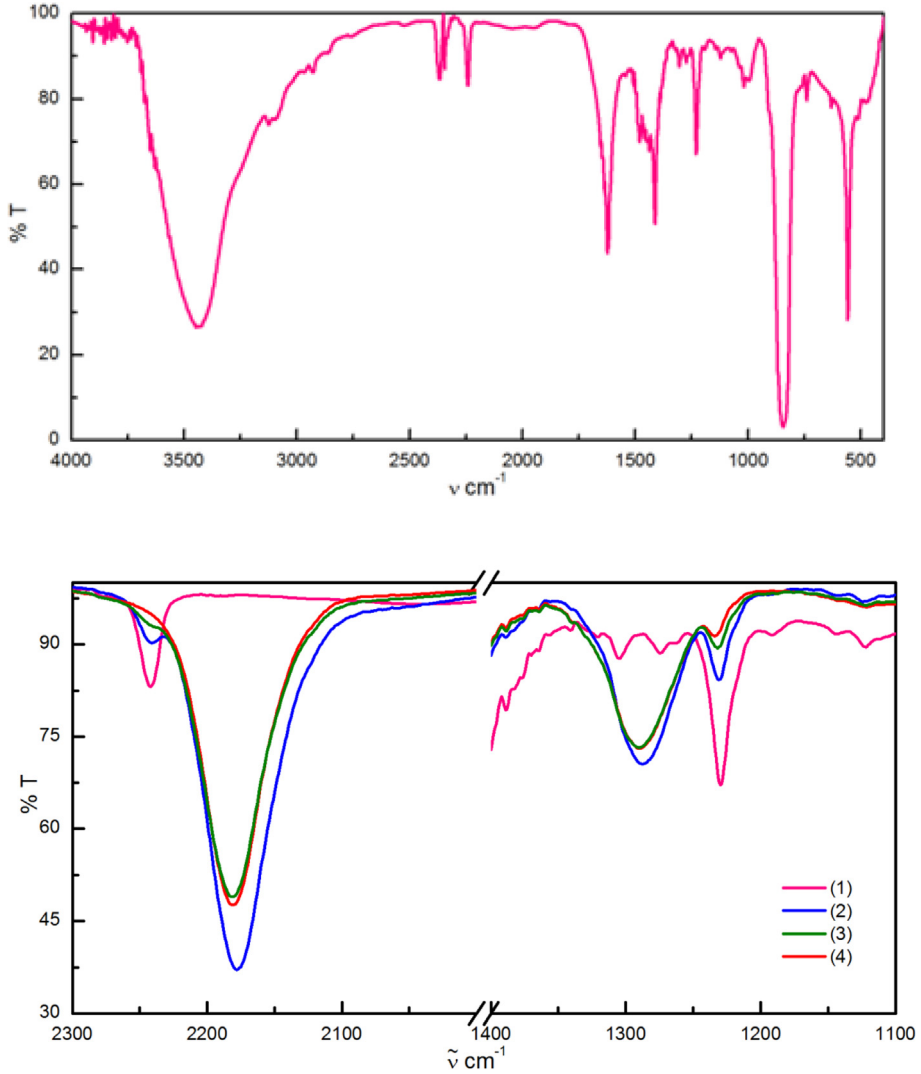

Fig. 1. *Above*: Normalized IR spectrum of (**1**). *Below:* Normalized IR spectra of (**1**), (**2**), (**3**) and (**4**) in the region corresponding to ν (C≡N) and $\delta_{sym}(NH_3)$ bands. All the spectra are normalized respect to the most intense band, ν (P-F) ≅ 830 cm^{-1}.

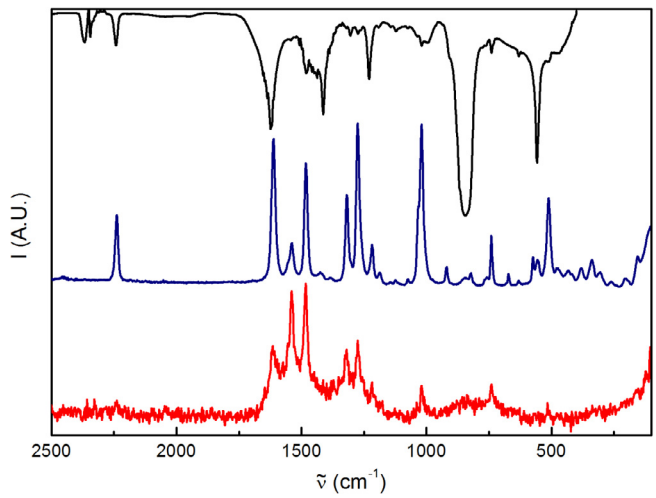

Fig. 2. IR spectrum (black), Resonance Raman spectrum (blue) – measured with a 532 nm laser – and Raman spectrum (red) – measured with a 780 nm laser- of complex (**1**). (Color online.)

corresponding to the C≡N stretching vibration. Considering that the totally symmetric modes that lead to the excited state configurations are most strongly resonance-enhanced in RR spectra [12], these results put into evidence the increased electronic delocalization over the bpy ring due to the nitrile moiety, in consistency with previous works that describe Mebpy-CN complexes with Ru [5] and Re [9].

3.3. Electrochemistry

Approximate values of the redox potentials obtained from cyclic and differential pulse voltammograms of complexes (**1**) to (**4**) in CH_3CN (0.1 M TBAH) are shown in Table 1. For all complexes, oxidation of the metallic centers are quasi-reversible. The values of the redox potentials of the $Fe^{3+/2+}$ couple increase along the series (**1**)–(**4**) from $E_{1/2}$ = 1.29 to 1.40 V, as expected by taking into account the increase in charge of the complexes from 2+ to 8+. On the other hand, the values of the redox potentials of the $Ru^{3+/2+}$ couple ($E_{1/2}$ ≅ 0.71 V) for species (**2**) to (**4**) are the typical expected ones for a nitrile-coordinated species of a pentaammineruthenium moiety [5,9] and are independent of the charge, indicating no coupling between the peripheric ruthenium ammines.

Table 1
Electrochemical data for complexes in CH_3CN, *vs.* Ag/AgCl (3 M KCl), at 23 °C.

Complex	$E_{1/2}$ ($Fe^{3+/2+}$)	$E_{1/2}$ ($Ru^{3+/2+}$)	$E_{1/2}$ ($L_1^{0/-1}$)	$E_{1/2}$ ($L_2^{0/-1}$)	$E_{1/2}$ ($L_3^{0/-1}$)	$E_{1/2}$ ($L_1^{-1/-2}$)
(**1**)	1.29		−0.95	−1.12	−1.33	−1.68
(**2**)	1.33	0.71	−0.97	−1.11	−1.32	−1.62
(**3**)	1.37	0.70	−1.05	−1.17	−1.34	−1.64
(**4**)	1.40	0.72	−1.12	−1.34	−1.50	−1.66

All the complexes exhibit four reduction processes corresponding to the one-electron reductions of the three Mebpy-CN ligands (L_1, L_2 and L_3) and a two-electron reduction of Mebpy-CN. For complex (**1**), the three first reductions are quasi-reversible and the fourth is almost completely irreversible. The number of quasi-reversible waves in CV decreases along the series (**2**) to (**4**) according to the increasing number of nitrile-coordinated ligands; since the charge of the complexes increases along this series, a higher probability of adsorption onto the electrode surface that influence the number of irreversible reduction waves is expected and consequently the values of $E_{1/2}$ informed for compound (**4**) have the least precision.

3.4. UV–Vis spectra

Fig. 3 shows the UV–Vis spectra for complexes (**1**)–(**4**) in CH_3CN. Bands appearing at λ_{max} *ca.* 254 and 307 nm for all complexes are assigned to $\pi \rightarrow \pi^*$ (Mebpy-CN) IL (intraligand) transitions [5]. The observed visible bands are similar to those of $[Fe(bpy)_3]^{2+}$, although the maxima of the bands corresponding to MLCT transitions $d\pi(Fe) \rightarrow \pi^*$(Mebpy-CN) are displaced to the red respect to the MLCT transition $d\pi(Fe) \rightarrow \pi^*$(bpy) in the parent complex (λ_{max} = 520 nm) [13] and decrease in energy when increasing the number of peripheral ruthenium ammines (λ_{max} = 546, 573, 574 and 581 nm for complexes (**1**) to (**4**) respectively). The first effect can be explained by the stabilization of the ligand-centered LUMOs (Lowest Unoccupied Molecular Orbitals) of Mebpy-CN as compared to bpy, due to the increased delocalization imposed by the electron withdrawing properties of the nitrile groups, as already detected in $[Ru(Mebpy\text{-}CN)_3]^{2+}$ [5]. The second effect is an increased stabilization of the LUMOs due to increasing charge, which is also reflected in the red shifting of the MLCT transitions $d\pi(Ru) \rightarrow \pi^*$(Mebpy-CN) ($\lambda_{max}$ = 477, 490 and 495 nm for complexes (**2**) to (**4**) respectively). The molar absorptivities at the band maxima of the MLCT $d\pi(Fe) \rightarrow \pi^*$(Mebpy-CN) transitions also increase with the nuclearity of the complex: $\varepsilon_{max} = 0.90 \times 10^4$, 1.85×10^4, 2.81×10^4 and $3.80 \times 10^4\ M^{-1}\ cm^{-1}$ for complexes (**1**), (**2**), (**3**) and (**4**) respectively. This growth is due to the influence that exert the increasing number of ruthenium chromophores with absorptions overlapping with the iron chromophore.

These assignments are consistent with the spectral changes observed in the spectrophotometric titration with Br_2 and the spectroelectrochemical measurements for all complexes. Fig. 4 shows the experimental data obtained for complex (**4**) as a representative example. The behavior is similar for all polynuclear complexes. Chemical or electrochemical complete oxidations of the Ru (II) centers produce the bleaching of the band centered at λ_{max} *ca.* 490 nm (corresponding to the MLCT $d\pi(Ru) \rightarrow \pi^*$(Mebpy-CN)), but

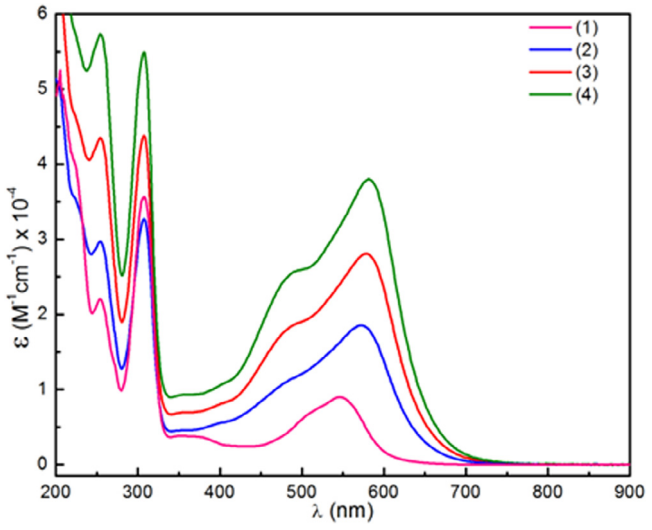

Fig. 3. UV–Vis spectra of (**1**) (pink line), (**2**) (blue line), (**3**) (orange line) and (**4**) (green line) in CH_3CN at r.t. (Color online.)

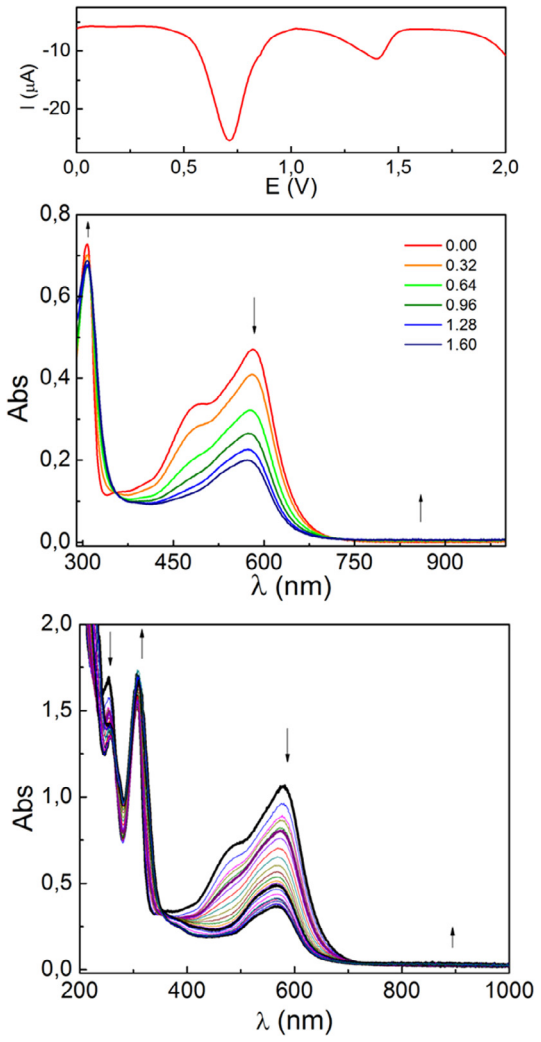

Fig. 4. *Above*: Differential Pulse Voltamperometry for (**4**) in CH_3CN, 0.1 M TBAH. *Middle:* spectrophotometric titration of (**4**) with Br_2 in CH_3CN; the legends indicate the $[Br_2]$/[Complex] ratio. *Below:* UV–Vis spectra obtained by controlled potential electrolysis of (**4**) up to 800 mV in CH_3CN, 0.1 M TBAH. All potentials are referred vs. Ag/AgCl.

the bands corresponding to the MLCT dπ(Fe) → π*(Mebpy-CN) are maintained at λ_{max} *ca.* 560 nm. The original spectra of the complexes are recovered by 75–90% by addition of the reducing agent $SnCl_2{\cdot}2H_2O$. The lower recovery proportion corresponds to (**4**) and the better one is determined for (**2**). Recovery in the electrochemical reduction is higher than 90% for all complexes.

As also shown in Fig. 4, oxidation of Ru(II) to Ru(III) induces the appearance of a new and low intensity band at $\lambda_{max} \cong 850$ nm, corresponding to an IVCT (intervalence charge transfer) or MMCT (metal-to-metal charge transfer) transition $d\pi(Fe^{II}) \rightarrow d\pi(Ru^{III})$, which will be discussed in the following section for complexes (**2**) to (**4**).

As concerning stability in CH_3CN, solutions of (**1**) are stable for several weeks, while solutions of the polynuclear complexes (**2**) to (**4**) are less stable; the latter one being the one that decomposes most rapidly (in several hours).

3.5. Intramolecular electron transfer

Spectroscopic and electrochemical data of complexes (**2**) to (**4**) confirm the coordination to the Ru center of one, two or three pentaammineruthenium moieties respectively of the free N of the nitrile group of Mebpy-CN bonded to Fe, as shown in Scheme 1. As already described in Section 3.4, selective oxidation of Ru in these complexes – either by a chemical or an electrochemical method – produces the mixed-valent complexes of formulae: $[(Mebpy\text{-}CN)_2Fe^{II}\ (Mebpy\text{-}CN)Ru^{III}(NH_3)_5]^{5+}$ or (**5**), $[(Mebpy\text{-}CN)Fe^{II}\{(Mebpy\text{-}CN)Ru^{III}(NH_3)_5\}_2]^{8+}$ or (**6**), and $[Fe^{II}\{(Mebpy\text{-}CN)Ru^{III}(NH_3)_5\}_3]^{11+}$ or (**7**). Fig. 5 (left side) shows the IVCT (or MMCT) bands that appear at $\lambda_{max} \cong 850$ nm for complexes (**5**) to (**7**), by oxidation by Br_2 vapor in CH_3CN of complexes (**2**) to (**4**) respectively. As expected, the intensities of the MMCT bands increase as the number of coordinated Ru centers increases: ε_{max} = 280, 650 and 941 $M^{-1}\ cm^{-1}$ for complexes (**5**), (**6**) and (**7**) respectively. Fig. 5 (right side) shows the electrochemical oxidation of (**4**) in the 700–1100 nm region.

The experimental values of $\tilde{\nu}_{max}$, $\Delta\tilde{\nu}_{1/2}$ and ε_{max}, where $\tilde{\nu}_{max}$ is the energy of the intervalence absorption maximum (in cm^{-1}), $\Delta\tilde{\nu}_{1/2}$ is the bandwidth at half-height of the intervalence transition (in cm^{-1}) and ε_{max} is the molar absorptivity at the band maximum (in $M^{-1}\ cm^{-1}$), can obtained by deconvolution of the Gaussian-shaped IVCT bands. These values can be used to calculate H_{AB}, α^2, and λ (electronic coupling in cm^{-1}, electron delocalization parameter, and reorganization energy in eV for the intramolecular IVCT, respectively) [14] through Eqs. (1) to (3):

$$H_{AB} = 2.06 \times 10^{-2}(\varepsilon_{max}.\tilde{\nu}_{max}.\Delta\tilde{\nu}_{1/2})^{1/2}(1/r) \quad (1)$$

$$\alpha^2 = (H_{AB}/\tilde{\nu}_{max})^2 \quad (2)$$

$$\lambda = E_{op} - \Delta G^0 - \Delta E_{exc} \quad (3)$$

where r is the separation between both metals (in Å), E_{op} is the energy of the IVCT maximum (in eV), ΔG^0 is the equilibrium free-energy difference between both metal redox centers - assumed as approximately $\Delta E_{½} = E_{½}(Fe^{3+/2+}) - E_{½}\ (Ru^{3+/2+})$ – and ΔE_{exc} is the energy difference between the excited and ground states, estimated as 0.25 eV for several ruthenium complexes in the event that the MMCT transition results in the population of an excited state [15]. The proposed metal–metal distance r for these complexes is 9.12 Å, as estimated by DFT geometry optimization for the mononuclear complex – carried out with a three parameter hybrid functional B3LYP and a LanL2DZ basis set as described before [5] – plus the typical crystallographic distance Ar–CN–$Ru(NH_3)_5$ [16]. Table 2 shows the experimental and calculated parameters for intramolecular electron transfer processes in complexes (**5**)–(**7**).

For the binuclear complex (**5**), the value of the estimated electronic coupling element H_{AB} is lower than that found in mixed-valent complexes with a similar metal–metal distance, of formula $[(bpy)_2Ru(Mebpy\text{-}CN)Ru(NH_3)_5]^{5+}$ [5] and $[(CH_3CN)(CO)_3Re(Mebpy\text{-}CN)Ru(NH_3)_5]^{4+}$ [9], indicating increased coupling when the period of the transition metal becomes larger.

On the other hand, increasing the number of π-accepting pentaammineruthenium (III) groups in the periphery of the iron complex produces a systematic increase of the electronic coupling and a decrease of the reorganization energy due to rising electronic delocalization. The values of the reorganization energy λ are less than those of $-\Delta G°$ for each complex; therefore, it can be predicted

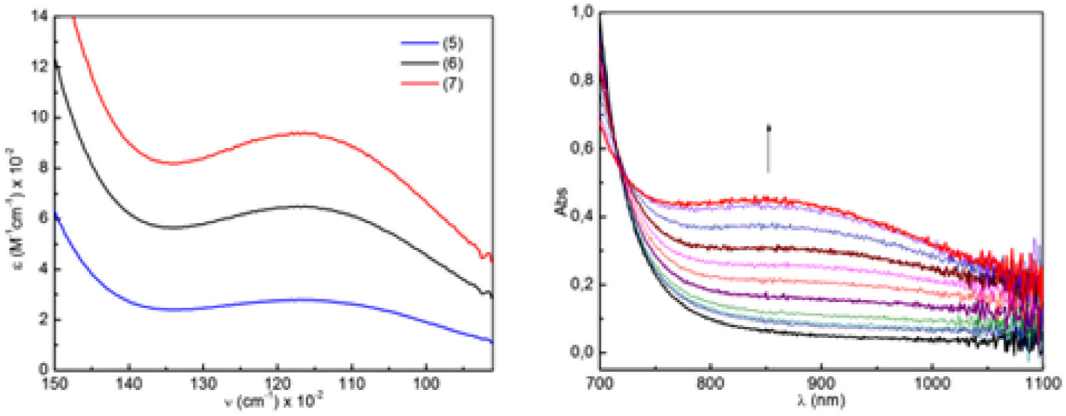

Fig. 5. Left: MMCT bands of (**5**), (**6**) and (**7**) in CH_3CN. Right: Visible spectra (in the 700–1100 nm region) obtained by controlled potential electrolysis of (**4**) up to 800 mV *vs.* Ag/AgCl in CH_3CN, 0.1 M TBAH.

Table 2
Parameters for intramolecular electron transfers.

Complex	$\tilde{\nu}_{max} \times 10^{-4}$ (cm^{-1})	$\Delta\tilde{\nu}_{1/2}$ (cm^{-1})	ε_{max} ($M^{-1}\ cm^{-1}$)	H_{AB} (cm^{-1})	$\alpha^2 \times 10^4$	λ (eV)
(**5**)	1.18	4890	280	287	5.92	0.59
(**6**)	1.18	4134	650	402	11.6	0.54
(**7**)	1.18	5122	941	539	20.9	0.53

that the rate constants for the charge-recombination step $Ru^{II} \rightarrow Fe^{III}$ following light excitation will fall in the Marcus inverted region [17], an important property of molecular systems capable of efficient energy conversion [18].

4. Conclusions

We conclude that introducing ruthenium ammines one at a time in the periphery of a novel iron bipyridyl complex containing three bridging ligands with nitrile groups can modulate the absorption coefficients in the visible region when using Ru(II) and in the NIR region when resorting to Ru(III). Both effects are proportional to the nuclearity of the complex and are relevant in improving the performance of Dye-Sensitized Solar Cells (DSSCs). In fact, since the ideal sensitizer in molecular photovoltaic devices should absorb all visible and NIR light below a threshold wavelength of about 900 nm [19], it can be predicted that sensitizers with nitrile groups as anchoring entities to semiconductors in DSSCs, such as those described recently [20], will be more efficient when incorporating pentaammineruthenium(II/III) entities in the periphery of the sensitizers.

Acknowledgements

We thank Universidad Nacional de Tucumán (UNT), Consejo Nacional de Investigaciones Científicas y Técnicas (CONICET), and Agencia Nacional de Promoción Científica y Tecnológica (ANPCyT), all from Argentina, for financial support. N.E.K. is a Member of the Research Career from CONICET, Argentina.

References

[1] C. Creutz, H. Taube, J. Am. Chem. Soc. 91 (1969) 3988.
[2] R.A. Marcus, Discuss. Faraday Soc. 29 (1960) 21.
[3] N. Hush, Trans. Faraday Soc. 57 (1961) 557.
[4] T.J. Meyer, Acc. Chem. Res. 22 (1989) 163.
[5] J.H. Mecchia Ortiz, N. Vega, D. Comedi, M. Tirado, I. Romero, X. Fontrodona, T. Parella, F.E. Morán Vieyra, C.D. Borsarelli, N.E. Katz, Inorg. Chem. 52 (2013) 4950.
[6] M.J. Powers, R.W. Callahan, D.J. Salmon, T.J. Meyer, Inorg. Chem. 15 (1976) 894.
[7] J.E. Sutton, H. Taube, Inorg. Chem. 20 (1981) 3125.
[8] F.R. Keene, Coord. Chem. Rev. 166 (1997) 121.
[9] J.H. Mecchia Ortiz, F.E. Morán Vieyra, C.D. Borsarelli, I. Romero, X. Fontrodona, T. Parella, N.D. Lis de Katz, F. Fagalde, N.E. Katz, Eur. J. Inorg. Chem. (2014) 3359.
[10] A. Yeh, A. Haim, M. Tanner, A. Ludi, Inorgan. Chim. Acta 33 (1979) 51.
[11] B.D. Alexander, T.J. Dines, R.W. Longhurst, Chem. Phys. 352 (2008) 19.
[12] J.R. Ferraro, K. Nakamoto, C.W. Brown, Introductory Raman Spectroscopy, second ed., Elsevier Ltd., 2003.
[13] P.S. Braterman, J.-I. Song, R.D. Peacock, Inorg. Chem. 31 (1992) 555.
[14] C. Creutz, Prog. Inorg. Chem. 30 (1983) 1.
[15] N.E. Katz, C. Creutz, N. Sutin, Inorg. Chem. 27 (1988) 1687.
[16] M.G. Mellace, F. Fagalde, N.E. Katz, I. Crivelli, A. Delgadillo, A.M. Leiva, B. Loeb, M.T. Garland, R. Baggio, Inorg. Chem. 43 (2004) 1100.
[17] R.A. Marcus, N. Sutin, Biochem. Biophys. Acta 811 (1985) 265.
[18] S. Fukuzumi, K. Ohkubo, T. Suenobu, Acc. Chem. Res. 47 (2014) 1455.
[19] A. Hagfeldt, M. Grätzel, Acc. Chem. Res. 33 (2000) 269.
[20] J.H. Mecchia Ortiz, C. Longo, N.E. Katz, Inorg. Chem. Comm. 55 (2015) 69.